Supplementary Information

Supplementary Methods

Mavárez *et al* 'Speciation by hybridization in *Heliconius* butterflies'.

Mate choice experiments: No-choice ML model [1]. A binomial mating probability $P_{i\,x\,j}$ was obtained for each combination of *i*-type female and *j*-type male, maximizing the expression for $\log_e$-likelihood given by:

$$m \log_e P_{i\,x\,j} + n \log_e (1 - P_{i\,x\,j})$$

where *m* and *n* are the numbers of trials in which the pair mated or remained unmated, respectively. The $\log_e$-likehoods for the $P_{i\,x\,j}$ values were maximized using the SOLVER algorithm supplied with Microsoft EXCEL. Support limits for $P_{i\,x\,j}$, which are asymptotically equivalent to 95% intervals, where obtained at the parameter values that led to a decrease in the $\log_e$-likelihood of two units.

Mate choice experiments: Colour Pattern Models ML model [2,3]. We estimated the probabilities $Q_{i\,x\,j}$ that males type *j* approached or courted models type *i* relative to that of their own type *j*, using likelihood and setting the model to one, so that any value under one represented preference for the control model. Thus, for M males with M versus C models, the actual probabilities are $Q_{A\,c\,x\,m}/(Q_{A\,c\,x\,m} + 1)$ that males approach C and $1/(Q_{A\,c\,x\,m} + 1)$ that they approach M. The $\log_e$-likelihood for this experiment is therefore $\sum[X_{A\,c\,x\,m} \log_e \{ Q_{A\,c\,x\,m}/(Q_{A\,c\,x\,m} + 1)\} + X_{A\,m\,x\,m} \log_e\{1/(Q_{A\,c\,x\,m} + 1)\}]$, where $X_{A\,c\,x\,m}$ is the number of M males approaching C and $X_{A\,m\,x\,m}$ is the number approaching M. Similarly Q_H *i* x *j* parameters were estimated for probability of hovering courtship of the model. The summed $\log_e$-likelihood was maximized over all experiments by varying the Q_H *i* x *j* parameters. Confidence intervals for parameters were established using the same likelihood method described for mating experiments.

References

1. Naisbit, R. E., Jiggins, C. D. & Mallet, J. Disruptive sexual selection against hybrids contributes to speciation between *Heliconius cydno* and *Heliconius melpomene*. *Proc. Roy. Soc. B.* **268**, 1849-1854 (2001).

2. Jiggins, C. D., Naisbit, R. E., Coe, R. L. & Mallet, J. Reproductive isolation caused by colour pattern mimicry. *Nature* **411**, 302-305 (2001).

3. Jiggins, C. D., Estrada, C. & Rodrigues, A. Mimicry and the evolution of premating isolation in *Heliconius melpomene* Linnaeus. *J. Evol. Biol.* **17**, 680-691 (2004).

4. Pritchard, J. K., Stephens, M. & Donnelly, P. J. Inference of population structure using multilocus genotype data. *Genetics* **155**, 945-959 (2000).

5. Clement MD, Posada D, Crandall KA (2000) TCS: a computer program to estimate gene genealogies. *Mol. Ecol*. **9**, 1657-1660.

6. Bookstein, F. L. *Morphometric Tools for Landmark Data: Geometry and Biology* (Cambridge University Press, Cambridge, 1991).

7. Adams, D. C., Rohlf, F. J. & Slice, D. E. Geometric Morphometrics: Ten Years of Progress Following the 'Revolution'. *Ital. J. Zool.* **71**, 5-16 (2004).

8. Rohlf, F. J. & Marcus, L. F. A revolution in morphometrics. *Trends Ecol. Evol.* **8**, 129-132 (1993).

9. Rohlf, F. J. & Slice, D. E. Extensions of the Procrustes method for the optimal superimposition of landmarks. *Syst. Zool.* **39**, 40-59 (1990)

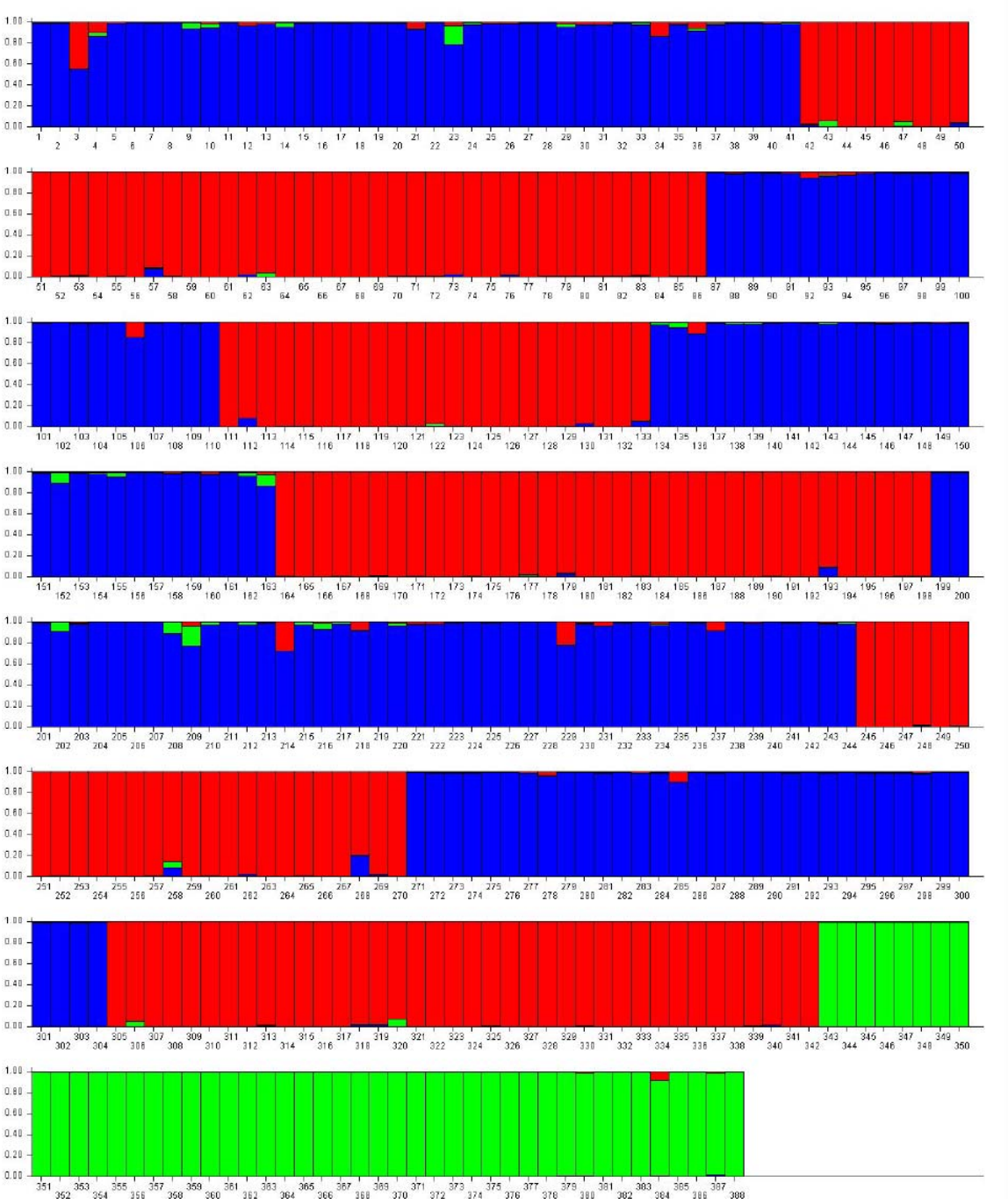

Supplementary Figure 1. Reproductive isolation between *H. cydno*, *H. melpomene* and *H. heurippa*. We used the software *Structure 2.1* [4] with the multilocus microsatellite data set to assign individuals to species and detect admixed individuals (*i.e.* hybrids). We ran *Structure 2.1* varying the burnin (10^4 to 10^5) and run length (10^5 to 10^6), number of clusters (1 to 4), ancestry type (with and without admixture) and allele frequency estimation (correlated and independent), in order to

obtain the highest probability model for the dataset. The figure shows the results obtained with the best model (three clusters, admixture and independent estimations of allele frequencies). The relative contribution of the three clusters to each individual's genome is shown in the Y axis. Blue: *H. cydno*, Red: *H. melpomene* and green: *H. heurippa*. Collection sites: Pipeline road, Panama (1-41 *H. cydno*, 42-86 *H. melpomene*); Parcela 33, Colombia (87-110 *H. cydno,* 111-133 *H. melpomene*); San Cristóbal, Venezuela (134-163 *H. cydno*, 164-198 *H. melpomene*); La Gira, Venezuela (199-244 *H. cydno*, 245-270 *H. melpomene*); Ocache, Colombia (271-304 *H. cydno*) and Villavicencio, Colombia (305-342 *H. melpomene*, 343-388 *H. heurippa*).

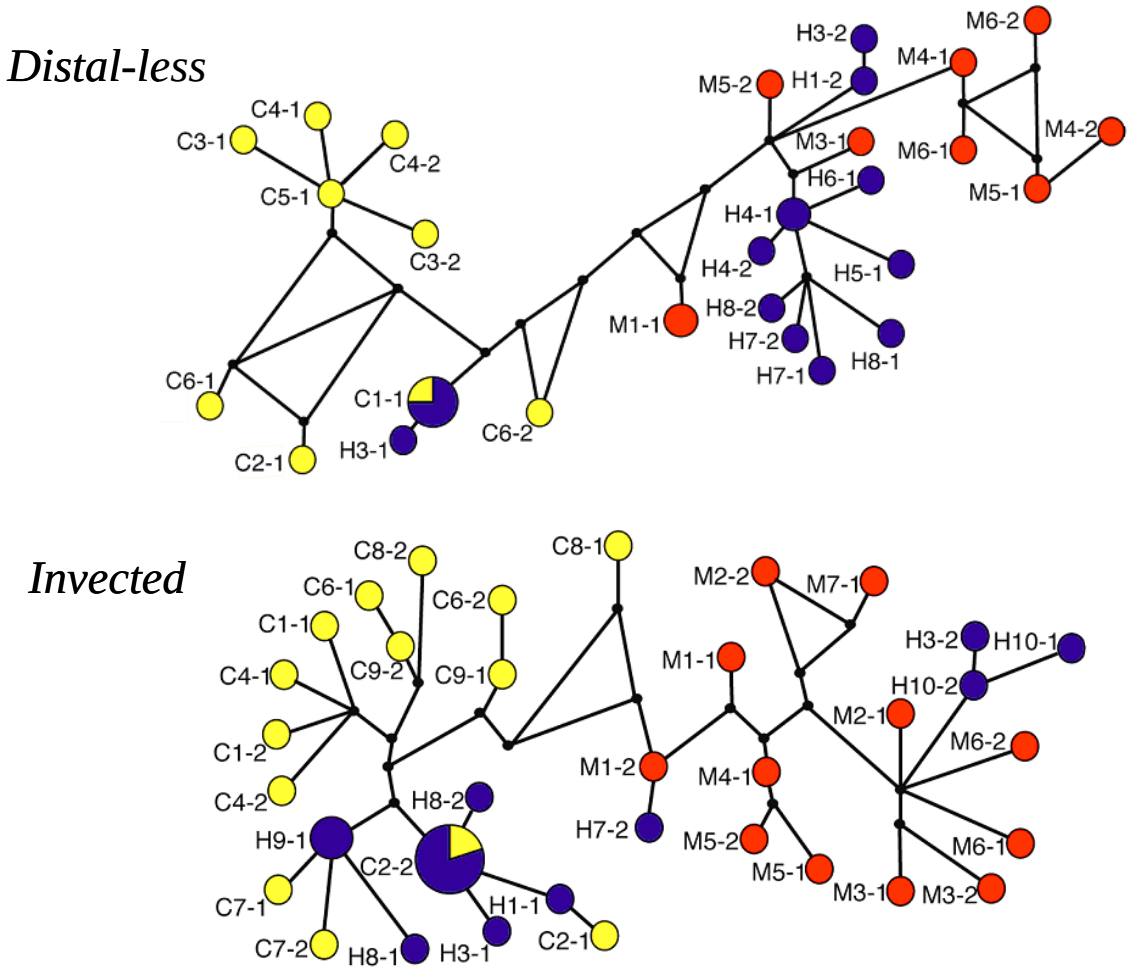

Supplementary Figure 2. Allele networks for nuclear genes (CS, CDJ and ML unpublished). Yellow, red and blue are *H. c. cordula*, *H. m. melpomene* and *H. heurippa* alleles. Respective alleles are identified with the letters C, M and H, followed by the individual number and allele number. Black dots are hypothetical ancestors. Sizes of the circles reflect allele frequencies in the population. Networks were constructed with statistical parsimony in TCS v 1.21 [5] (a method that allows the identification of putative recombination events by looking at the spatial distribution in the sequence of the homoplasies defined by the network), considering gaps as missing data and adjusting the parsimony limit to the respective data set.

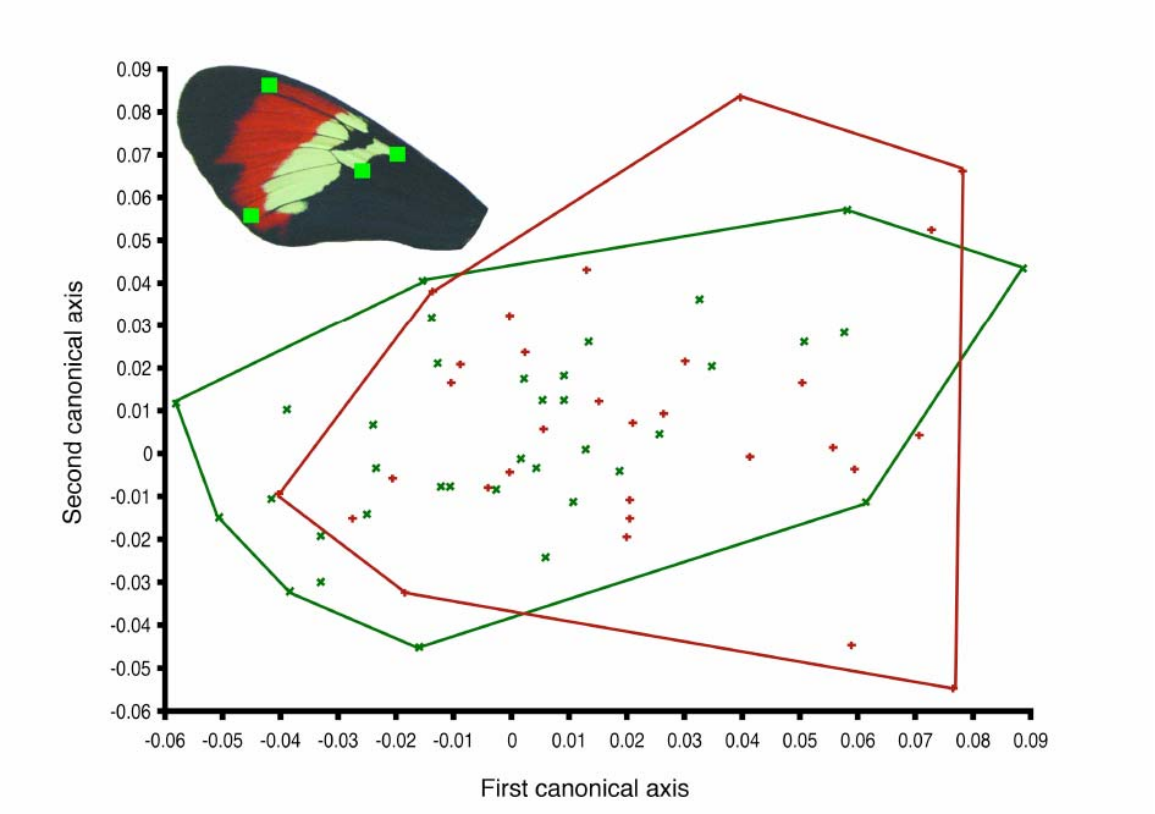

Supplementary Figure 3. Morphological comparison of reconstructed hybrids and wild *H. heurippa*. The shape of the forewing band was studied in 30 *H. heurippa* females and 37 *H. heurippa*-like lab hybrid females, using geometric morphometrics methods [6-8]. We took X,Y coordinates of four homologous landmarks that describe the general shape of the forewing band in scanned pictures of wings. The variation unexplained by the shape of the forewing band was removed using Generalized Procrustes Superimposition [7,9]. The canonical analysis of variance (CAV) used to test for significant differences in the shape of the forewing band between wild *H. heurippa* and *H. heurippa*-like lab hybrids found no differences in the wing pattern shapes of the two groups (Wilk's Lambda = 0.9046, p = 0.1768).

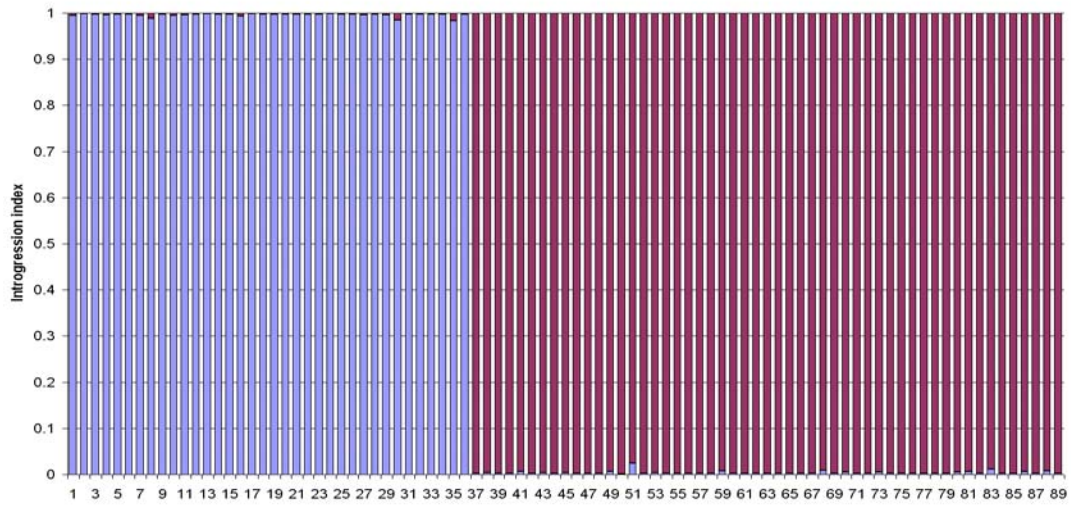

Supplementary Figure 4. Introgression analysis of *H. cydno* and *H. melpomene* at San Cristóbal, Venezuela. The same microsatellite loci described in **Methods** were scored in 36 *H. melpomene* (ind. 1 to 36), 44 *H. cydno* (ind. 37 to 80) and 9 hybrids (ind. 81 to 89) from Paramillo Natural Park, San Cristóbal, Venezuela. We used the software *Structure 2.1* [4], in order to assign individuals to species and to detect admixed individuals (*i.e.* hybrids), based on their multilocus microsatellite genotype. We varied the burnin (10^4 to 10^5), run length (10^5 to 10^6), number of clusters (1 to 4), ancestry type (with and without admixture) and allele frequency estimation (correlated and independent), in order to obtain the highest probability model for the dataset (which was obtained with two clusters, admixture and independent estimations of allele frequencies). The contribution of each cluster to each individual's genome was used as an introgression index, useful to describe its genotypic class. For example, F_1, first-, second-, third- and fourth-generation backcrosses to *H. cydno* should have, on average, 50%, 25%, 12.5%, 6.25% and 3.13% of their genome introgressed from *H. melpomene*, respectively. Colours represent the contribution of each species-cluster (blue: *H. melpomene*, red: *H. cydno*) to the introgression index. The hybrid individuals cannot be distinguished from other individuals of *H. cydno*, indicating that multiple generations of backcrossing must have occurred.

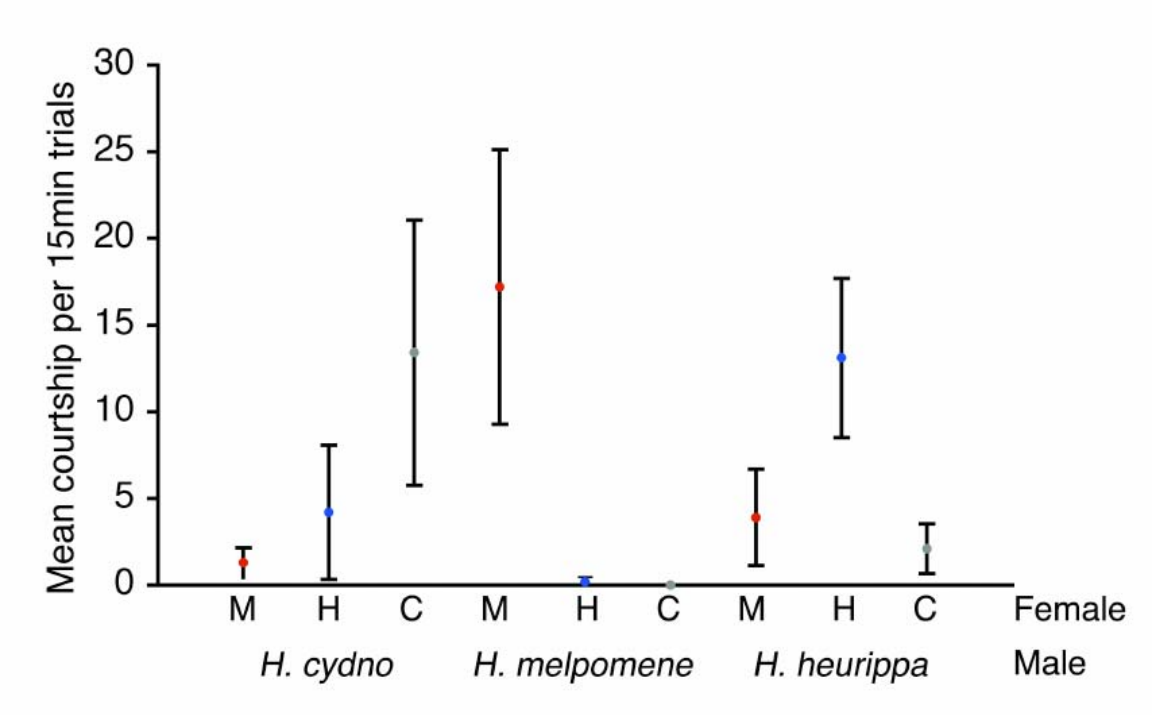

Supplementary Figure 5. Live courtship experiments. We placed mature males (> 5 days old) of each genotype in an insectary and introduced a single virgin female (1-5 days old). The number of courtship bouts (sustained hovering by the male over the female) occurring over a period of 15 minutes was recorded. The female genotype was then substituted, with genotype order randomized, such that each panel of males was tested against each female genotype. No mating was permitted in order to not disrupt subsequent behaviour. Males were used only once. In total 30 replicate panels of males were tested against all three female genotypes in more than 450 min of observations. *H. melpomene* (red dots), *H. heurippa* (blue dots) and *H. cydno* (grey dots).

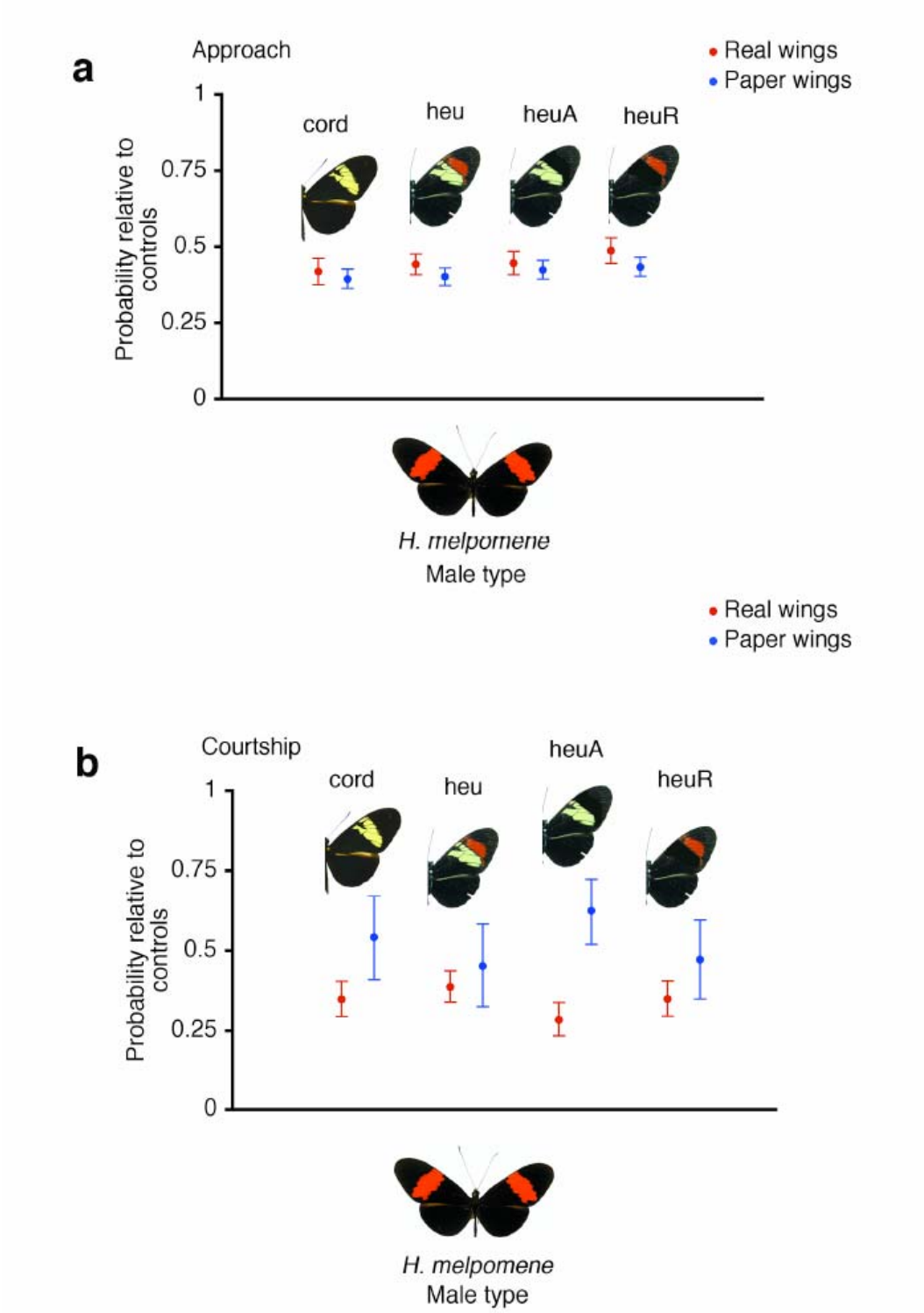

Supplementary Figure 6. Colour pattern models for *H. melpomene*. Model experiments were carried out as described in **Methods** using *H. melpomene* males. In all comparisons, males of *H. melpomene* prefer to approach and court the real wings and paper models of their own phenotype.

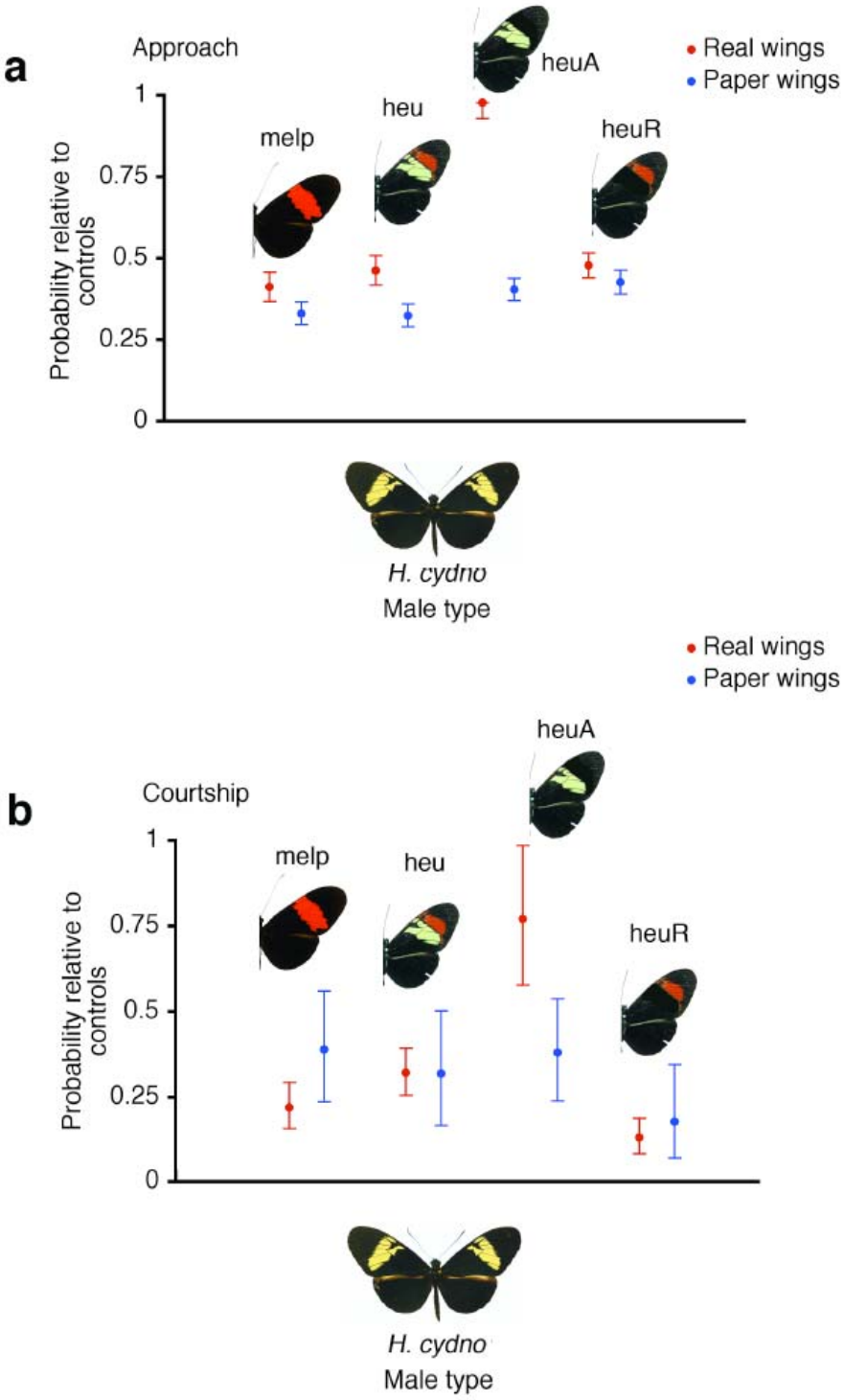

Supplementary Figure 7. Colour pattern models for *H. cydno* males. Model experiments were carried out as described in **Methods** using *H. cydno* males. *H. cydno* prefer to approach and court the real wings and paper models of their own phenotype and real wings of *H. heurippa* with the red band removed.

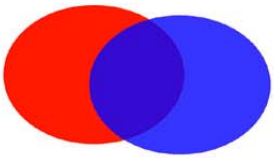

H. cydno and *H. melpomene* overlap and hybridise occasionally, but hybrids are eliminated by predator selection.

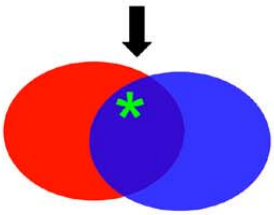

A local reduction in selection leads to the establishment of a polymorphic population resulting from backcrossing of *H. melpomene* genes into a *H. cydno* background (e.g. as currently observed in San Cristóbal, Venezuela).

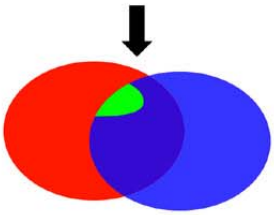

The return of selection favours the most abundant hybrid form and drives it to fixation. This result in a "proto-*H. heurippa*" pattern established as a parapatric race of *H. cydno*. This race is sympatric with *H. melpomene*, from which it is isolated by partial sterility and weak assortative mating.

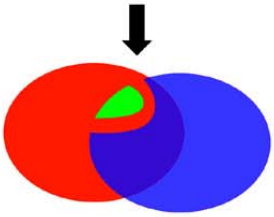

Mate preference diverges in the proto-*H. heurippa* race, such that its novel pattern is used as a cue in mate finding, leading to assortative mating with both parental species.

Supplementary Figure 8. A model for the hybrid origin of *Heliconius heurippa*.